

Cite this: *New J. Chem.*, 2011, **35**, 1730–1739

www.rsc.org/njc

PAPER

Rhodium(I) complexes bearing N-donor ligands: catalytic activity towards intramolecular cyclization of alkynoic acids and ligand lability†

Bradley Y.-W. Man,^a Mohan Bhadbhade^{ab} and Barbara A. Messerle^{*a}

Received (in Gainesville, FL, USA) 5th February 2011, Accepted 2nd June 2011

DOI: 10.1039/c1nj20094a

The structures of rhodium(I) complexes bearing tris(pyrazol-1-yl)toluidine (tpt) and tris(*N*-methylimidazol-2-yl)methanol (tim) ligands were examined in the solid state using single crystal X-ray diffraction, and in the solution state using variable temperature NMR spectroscopy. The solid state structures of the rhodium(I) tpt and rhodium(I) tim complexes showed that the ligands are bound to the rhodium(I) centre in the κ^2 binding mode, rather than the κ^3 binding mode. In the solution state, rhodium(I) complexes bearing the tpt ligand undergo fluxional behaviour at room temperature, which was attributed to rotation of the toluidine substituent about the C–C bond or the equilibrium between κ^2 and κ^3 binding modes. At low temperatures, rhodium(I) complexes bearing the tpt ligand adopted the κ^2 binding mode, consistent with the coordination mode in the solid state structures. The efficiency of the complexes as catalysts for the intramolecular hydroalkoxylation of 4-pentynoic acid and 5-hexynoic acid to form the corresponding lactone was established. The presence of the third unbound N-donor was shown to reduce the catalytic efficiency of the complexes with tridentate ligands when compared to their counterparts bearing bidentate ligands, due to either the steric hindrance or competitive binding of the third N-donor with the substrate during the catalytic cycle.

Introduction

Late transition metal complexes with polydentate *N*-donor ligands have been successfully used as catalysts for a wide range of transformations, including the formation of new bonds such as C–X bonds (X = N, O or S)¹ and hydroformylation.² Where phosphine and carbene donors are widely used as donors in late transition metal catalysts, the advantages of *N*-donor ligands lie in their synthetic accessibility and stability. Many of the *N*-donor ligands used in successful catalysts contain sp²-hybridised nitrogen donor atoms, including *N*-heterocyclic and diimine compounds. They are generally coordinated as multidentate ligands in order to reduce the lability of the metal–nitrogen bond.

The anionic poly(pyrazol-1-yl)borate ligands containing the pyrazolyl *N*-donor are widely used in coordination chemistry,³ and the poly(pyrazol-1-yl)methane and poly(imidazole-2-yl)methane ligands are neutral analogues of these.⁴ The coordination chemistry and catalytic activity of Group 9 complexes bearing

bis(pyrazol-1-yl)methane (bpm) ligands and bis(*N*-methylimidazol-2-yl)methane (bim) ligands are well studied.⁵ Although Group 9 complexes of the bidentate pyrazolyl and imidazolyl methane containing ligands are well studied, the complexes of their corresponding tridentate counterparts are not. The presence of the additional donor in the tridentate ligands could lead to different reactivities of the metal complexes due to changes in the coordination chemistry. Complexes bearing the tris(pyrazol-1-yl)toluidine ligand (**1**) have the potential to be immobilised onto macroscopic scaffolds such as polymers,⁶ silicon⁷ and proteins.⁸ Liddle *et al.*⁹ recently published a convenient synthesis for an amine functionalised tris(pyrazol-1-yl)alkane ligand, tris(pyrazol-1-yl)toluidine (tpt, Fig. 1).

Cationic rhodium(I) and iridium(I) complexes bearing bidentate *N*-donor ligands such as bpm are efficient catalysts for the formation of C–N¹⁰ and C–O¹¹ bonds. More specifically,

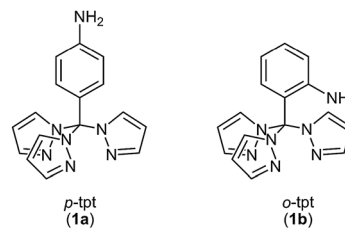
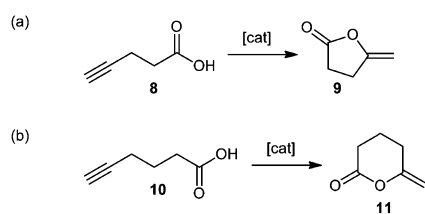


Fig. 1 The structures of tris(pyrazol-1-yl)toluidine ligands, *p*-tris(pyrazol-1-yl)toluidine (*p*-tpt, **1a**) and *o*-tris(pyrazol-1-yl)toluidine (*o*-tpt, **1b**) respectively.

^a School of Chemistry, University of New South Wales, Sydney, NSW 2052, Australia. E-mail: b.messerle@unsw.edu.au; Fax: +61-2-9385-6141

^b Mark Wainwright Analytical Centre, University of New South Wales, Sydney, NSW 2052, Australia

† Crystallographic data in CIF format for complexes **4b** (CCDC 782080), **6** (CCDC 782081), **2a** (CCDC 782082, 782083), **5** (CCDC 782085), **3b** (CCDC 782086), **3a** (CCDC 782087). For crystallographic data in CIF or other electronic format see DOI: 10.1039/c1nj20094a



Scheme 1 Catalysed intramolecular cyclization of: (a) 4-pentynoic acid (**8**); and (b) 5-hexynoic acid (**10**) to the corresponding cyclic lactones **9** and **11**, respectively.

Rh(I) complexes with sp^2 -N donor ligands¹² and cationic Rh/Ir(I) complexes of the tris-carbene (TIMEN) tris[2-(3-isopropylimidazol-2-ylidene)ethyl]amine ligand system¹³ are efficient catalysts for the intramolecular cyclisation of acetylenic carboxylic acids. The transition metal catalysed intramolecular cyclisation of acetylenic carboxylic acids offers an atom efficient approach to the synthesis of five and six-membered ring systems containing oxygen.¹⁴ Industrially, this catalytic process is particularly useful for the preparation of pharmaceuticals, flavours and fragrances.¹⁵ The Rh,^{12,13,16} Pd^{16a} and Hg¹⁷ catalysed intramolecular cyclisation of alkynyl carboxylic acids forming the five-membered or six-membered exocyclic enol lactones has been performed previously (Scheme 1).

Here, the structures of a series of rhodium(I) tris(pyrazol-1-yl)toluidine complexes bearing a range of co-ligands were investigated. The structures of the analogous Rh(I) complexes bearing tris(*N*-methylimidazol-2-yl)methanol ligands were also investigated. In order to establish the effect the presence of a third sp^2 *N*-donor or a toluidine substituent on the ligand may have on the catalytic activity of the Rh(I) complexes, we compared the catalytic efficiency of the rhodium(I) complexes bearing the tridentate ligands described here with that of their counterparts bearing bidentate ligands for the intramolecular cyclization of the aliphatic alkynoic acids **8** and **10**.

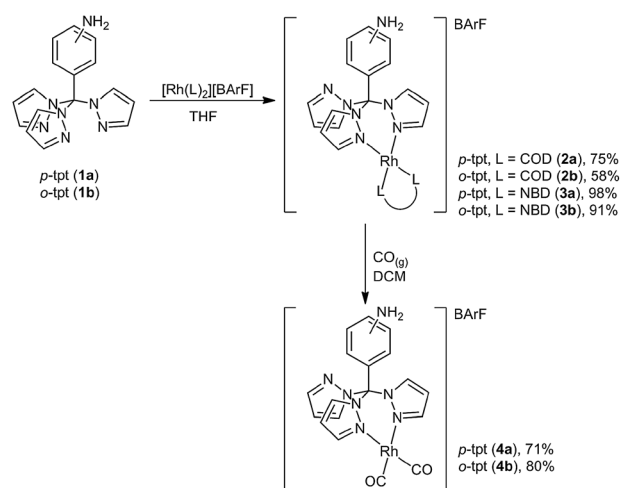
Results and discussion

Synthesis of rhodium(I) complexes bearing tris(pyrazol-1-yl)toluidine ligands (**1**)

The rhodium(I) tris(pyrazol-1-yl)toluidine olefin complexes (**2** and **3**) were synthesised by stirring a solution of $[Rh(L)_2][BARF]$ ($L = 1,5$ -cyclooctadiene, COD; or norbornadiene, NBD) with the appropriate ligand (**1**) in tetrahydrofuran (THF) at room temperature (Scheme 2). The bisolefin complexes (**2** and **3**) were isolated and purified by the removal of THF *in vacuo*, followed by recrystallisation from a mixture of dichloromethane and *n*-pentane. The corresponding dicarbonyl complexes **4** (**a** and **b**) were synthesised by stirring a degassed solution of the olefin complex **2** in dichloromethane under a carbon monoxide (CO) atmosphere. The resulting dicarbonyl complexes **4** were isolated by the addition of *n*-pentane followed by recrystallisation from dichloromethane and *n*-pentane.

Solid state structures of rhodium (I) complexes bearing the tris(pyrazol-1-yl)toluidine ligand (**1**)

Single crystals of complexes **2a**, **2b**, **3a**, **3b** and **4b** suitable for X-ray diffraction analysis were grown by the slow diffusion of



Scheme 2 Synthesis of rhodium (I) complexes **2–4** bearing the tpt ligand (**1**).

n-pentane into a concentrated solution of the desired complex in dichloromethane at room temperature. The crystals were analysed using single crystal X-ray diffraction and the crystallographic parameters are summarized in Table 1. Selected bond lengths and angles for the complexes **2a**, **2b**, **3a**, **3b** and **4b** are shown in Table 2. ORTEP depictions of the cationic fragments of the complexes are shown in Fig. 2 (**2a** and **3a**), Fig. 3 (**2b**), Fig. 4 (**3b**) and Fig. 5 (**4b**).

All of the rhodium(I) complexes bearing the tpt ligand (**1**) and cyclic bisolefins as co-ligands adopted a distorted square planar geometry around the rhodium(I) centre. The molecular structure (Fig. 2(a)) of $[Rh(COD)(p\text{-tpt})][BARF]$ (**2a**) shows the *p*-tpt ligand (**1a**) coordinated to the rhodium(I) centre *via* the κ^2 binding mode. The unbound pyrazolyl donor in complex **2a** is positioned away from the rhodium centre with the phenyl ring of the *p*-tpt ligand (**1a**) above the rhodium centre. To reduce the steric interactions between the co-ligand and the *p*-tpt ligand (**1a**) the smaller and more constrained co-ligand norbornadiene was also used. The molecular structure of the resulting complex $[Rh(NBD)(p\text{-tpt})][BARF]$ (**3a**) shows that the *p*-tpt ligand (**1a**) was also bound to the rhodium centre *via* κ^2 binding mode in this complex. Increased N–Rh–X bite angle values observed for the NBD complex **3a** compared to those of the COD complex **2a** are attributed to the reduced Rh–N bond lengths and the more constrained nature of the NBD co-ligand.

In the tris(3,5-dimethylpyrazol-1-yl)methane complexes of Rh(I) reported previously by Hallett *et al.*,¹⁸ the use of a smaller and more constrained co-ligand such as NBD led to a significant change in the coordination geometry of the tris(pyrazol-1-yl)methane ligands, with the tridentate ligand changing from the κ^2 binding mode to the κ^3 binding mode. This was attributed to a reduction in the steric interaction between the *N*-donor ligand and bisolefin co-ligand. This was also observed in the complexes reported by Adams *et al.*¹⁹ where the smaller CO co-ligand led to the κ^3 binding mode of the tridentate *N*-donor ligands in the solution phase. These observations suggest that in the case of the tpt ligand under investigation here, steric interactions between the co-ligand and the *N*-donor ligand are not solely responsible for the dominance of the κ^2 binding mode. This in turn suggests that the presence of an

Table 2 Selected bond lengths and angles for the complexes **2a**, **2b**, **3a**, **3b** and **4b**

Atom Pairs	[Rh(COD)(<i>p</i> -tpt)]-[BArF] (2a)	[Rh(NDB)(<i>p</i> -tpt)]-[BArF] (3a)	[Rh(COD)(<i>o</i> -tpt)][BArF] (2b)		[Rh(NBD)(<i>o</i> -tpt)]-[BArF] (3b)	[Rh(CO) ₂ (<i>o</i> -tpt)]-[BArF] (4b)
			A	B		
	Bond lengths (Å)					
Rh–N1	2.104(3)	2.056(6)	2.065(6)	2.099(6)	2.056(6)	Rh–N1 2.052(3)
Rh–N2	2.102(3)	2.036(7)	2.099(7)	2.086(7)	2.036(7)	Rh–N2 2.086(3)
Rh–X1 ^a	2.015	2.001	2.018	2.018	1.995	Rh–C1 1.851(5)
Rh–X2 ^a	2.024	2.009	2.008	2.002	1.983	Rh–C2 1.847(4)
	Bond angles (°)					
N1–Rh–X1	93.06	101.05	95.60	95.32	98.87	N1–Rh–N2 85.71(11)
N2–Rh–X2	94.89	100.82	93.10	93.27	101.97	C1–Rh–C2 88.03(17)
N1–Rh–N2	84.89(11)	86.28(13)	86.10(3)	86.40(2)	88.20(2)	N1–Rh–C1 92.16(16)
X1–Rh–X2	87.28	71.72	86.57	86.65	71.16	N2–Rh–C2 94.04(14)

^a X1 and X2 are defined as the centroids for the alkene bonds of the COD and NBD co-ligands.

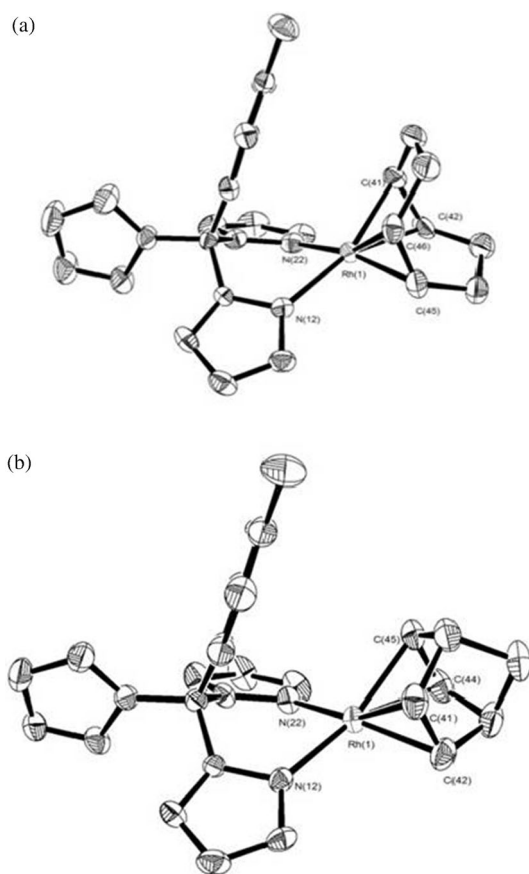


Fig. 2 ORTEP depictions of the cationic fragments of (a) [Rh(COD)(*p*-tpt)][BArF] (**2a**) and (b) [Rh(NBD)(*p*-tpt)][BArF] (**3a**) at 50% thermal ellipsoid for non-hydrogen atoms.

to either exchange between the κ^3 and κ^2 binding mode or atropisomerism, which would involve the rotation of the toluidine ring about the C–C bond connecting the toluidine ring to the bridging carbon. Upon cooling to -50°C , the signals in the NMR spectrum become sharper with the resonances due to the pyrazole H³, H⁴ and H⁵ protons each resolving into two resonances integrating to a ratio of 1:0.5 (Fig. 6(b)). This shows that there are two equivalent pyrazolyl donors in one environment, with the third pyrazolyl donor in a different chemical environment, which is consistent with the solid state

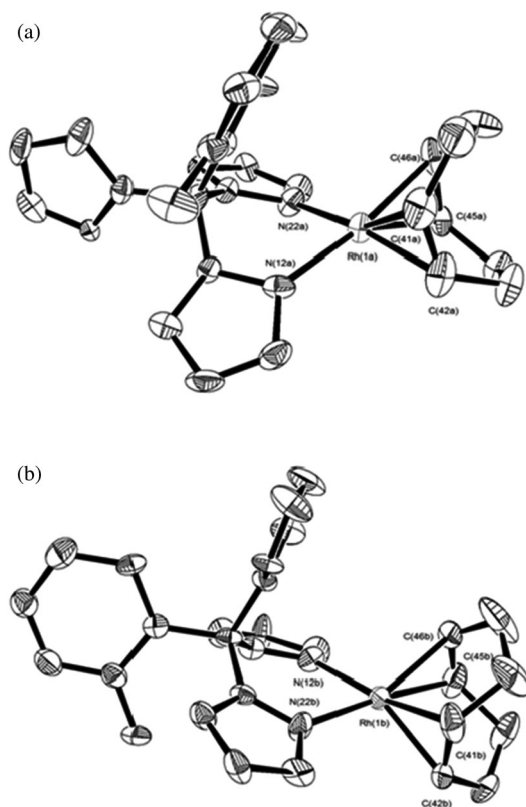


Fig. 3 ORTEP depictions showing the cationic fragment of the two co-crystallised structures for the complex [Rh(COD)(*o*-tpt)][BArF] (**2b**): (a) Structure A; and (b) Structure B, at 50% thermal ellipsoid for non-hydrogen atoms.

structure of the complex **2a**. The same observations were made for the corresponding NBD complex (**3a**) and the dicarbonyl complex (**4a**) of the *p*-tpt ligand.

The ¹H NMR spectrum of [Rh(COD)(*o*-tpt)][BArF] (**2b**), was similar to that of [Rh(COD)(*p*-tpt)][BArF] (**2a**), with broad resonances due to the pyrazolyl protons at room temperature, which sharpened upon cooling. However, in the case of the spectrum of **2b**, each of the resonances due to pyrazolyl protons resolved at low temperature into three distinct resonances, indicating that at low temperature there is no symmetry about the rhodium centre in **2b**, leading to three distinct pyrazolyl donor environments. In addition to the asymmetric pyrazolyl

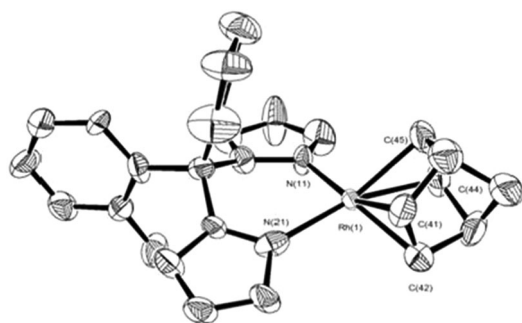


Fig. 4 ORTEP depiction of the cationic fragment of $[\text{Rh}(\text{NBD})(o\text{-tpt})]$ - $[\text{BARf}]$ (**3b**) at 50% thermal ellipsoid for non-hydrogen atoms.

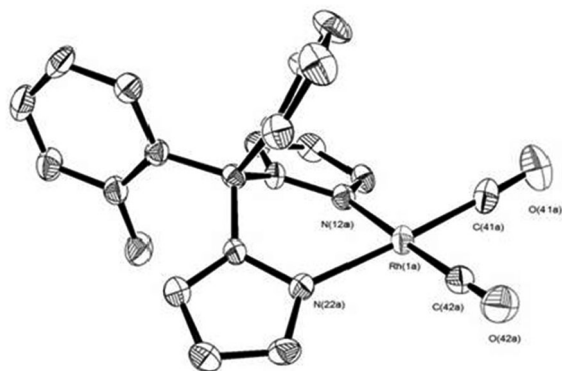


Fig. 5 ORTEP depiction of the cationic fragment of $[\text{Rh}(\text{CO})_2(o\text{-tpt})]$ - $[\text{BARf}]$ (**4b**) at 50% ellipsoid for non-hydrogen atoms.

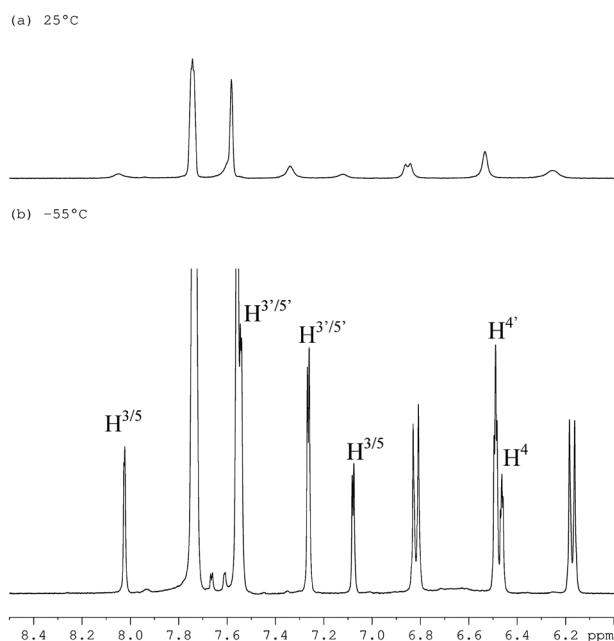


Fig. 6 ^1H NMR (600 MHz) spectrum of the complex **2a**: (a) at 25 °C; and (b) at -55 °C in CD_2Cl_2 showing only the aromatic region.

donor environment, a second minor species with similar chemical shifts and multiplicity was observed in the ^1H NMR spectrum at low temperatures (Fig. 7). This was indicated, for example, by the appearance of a low intensity second doublet, assigned

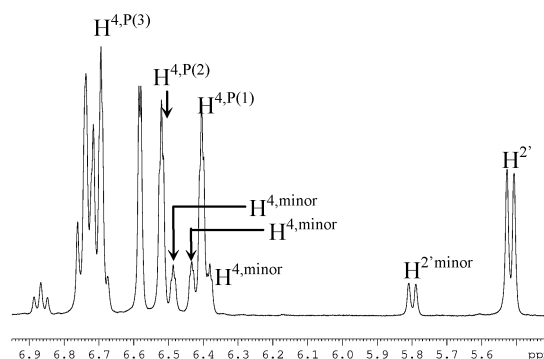


Fig. 7 ^1H NMR (600 MHz) spectrum of the complex **2b** at -55 °C in CDCl_3 showing only the aromatic region.

as the $\text{H}^{2'}$ proton on the aniline ring at 5.8 ppm. The resonances were fully assigned for both the major and minor products. An analogous minor species was also observed for the dicarbonyl complex **4b**. Elemental analysis of the complexes **2b**, **3b** and **4b** confirmed the purity of each of the complexes, suggesting that these minor species were the result of conformational exchange. The NOESY spectrum of **2b** at -50 °C (not shown) contained cross peaks due to exchange between the major and minor species showing that the second minor species arises due to conformational exchange. The two possible exchange processes giving rise to the second species could be interconversion between the κ^2 and κ^3 or atropisomerism.

In the work by Hallett *et al.*,¹⁸ it was shown for rhodium(i) coordinated to the tris(3,5-dimethylpyrazol-1-yl)methane ligand in a κ^2 binding mode, the ^{13}C chemical shift of the bridging carbon lies between 74–75 ppm, while for complexes where the rhodium is bound in the κ^3 binding mode the ^{13}C chemical shift of the bridging carbon lies between 67–70 ppm. Using an ^1H - ^{13}C HMBC correlation experiment, the resonances due to the bridging carbon for both the major and minor product of the complex **4b** were assigned. The ^{13}C chemical shifts of the bridging carbons for the major (92.8 ppm) and minor (93.0 ppm) products respectively differ by only 0.2 ppm. When compared to the 7 ppm difference observed by Hallett *et al.*¹⁸ between the rhodium(i) κ^2 and κ^3 complexes bearing the tris(3,5-dimethylpyrazol-1-yl)methane ligand, this suggests that the exchange being observed in the ^1H NMR spectra for complexes **2b**, **3b** and **4b** is due to atropisomerism, not exchange between κ^2 and κ^3 , with rotation of the toluidine substituent about the C–C bond between the bridging carbon of the ligand and the aryl carbon of the toluidine ring.

Synthesis of rhodium(i) complexes bearing tris(*N*-methylimidazol-2-yl)methanol ligands

The complexes $[\text{Rh}(\text{COD})(\text{tim})][\text{BARf}]$ (**5**) and $[\text{Rh}(\text{CO})_2(\text{tim})][\text{BARf}]$ (**6**) were synthesised using the same general synthetic strategy described above shown in Scheme 1 in 70% and 57% yield, respectively.²⁰

Solid and solution state structures of rhodium(i) complexes bearing the tris(*N*-methylimidazol-2-yl)methanol ligands

Single crystals of the complexes **5** and **6** were grown by the slow diffusion of *n*-pentane into a concentrated solution of

the complex in dichloromethane. The molecular structures for both complexes showed the rhodium centre coordinated to the tim ligand in κ^2 binding mode (the molecular structure of **5** is not shown). Unlike the rhodium(I) complexes bearing the tpt ligands, the NMR spectra of **5** did not show any fluxional behaviour at room temperature.

The solid state structure of $[\text{Rh}(\text{CO})_2(\text{tim})][\text{BArF}]$ (**6**) (Fig. 8, Table 3) shows that the rhodium centre binds to the tim ligand in κ^2 binding mode. The unit cell for the crystal structure of **6** shows two of the cationic fragments associated in space as indicated by the ORTEP representation viewed from the top (Fig. 8(a)) and the side (Fig. 8(b)). The two rhodium centres are located directly above each other with the distance between the two rhodium centres at 3.2 Å. This distance is longer than literature reported Rh–Rh bonds which are of the order of 2.3 Å.²¹

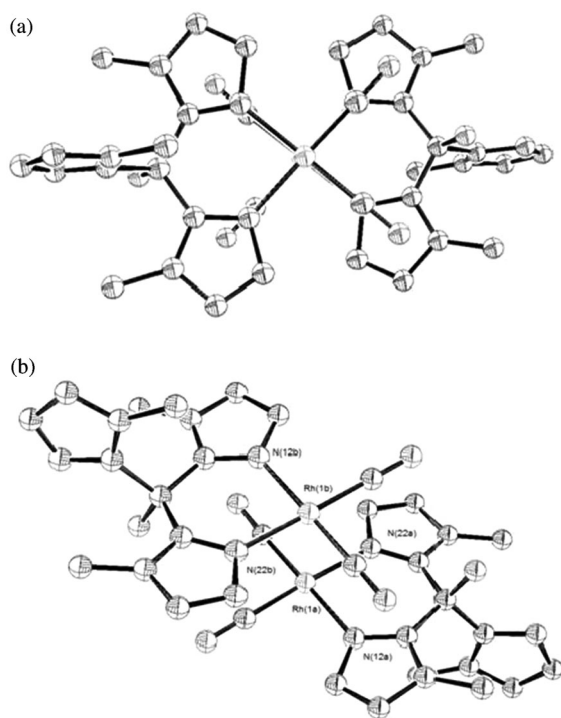


Fig. 8 ORTEP representation of the cationic fragment of the complex **6** at 50% ellipsoid for non-hydrogen atoms viewed from: (a) the side; (b) the top.

Table 3 Selected bond lengths and angles for the complexes **5** and **6**^a

Atom pair	$[\text{Rh}(\text{COD})(\text{tim})][\text{BArF}]$ (5) Bond lengths (Å)	Atom pair	$[\text{Rh}(\text{CO})_2(\text{tim})][\text{BArF}]$ (6) Bond lengths (Å)
Rh–N1	2.088 (4)	Rh–N1	2.048 (9)
Rh–N2	2.084 (4)	Rh–N2	2.072 (7)
Rh–X1	2.135	Rh–C1	1.839 (11)
Rh–X2	2.124	Rh–C2	1.851 (13)
	Bond angles (°)		Bond angles (°)
N1–Rh–N2	86.23 (14)	N1–Rh–N2	86.8(3)
X1–Rh–X2	86.42	C1–Rh–C2	85.5(5)
N1–Rh–X1	94.24	N1–Rh–C1	94.2(4)
N2–Rh–X2	92.80	N2–Rh–C2	93.7(4)

^a X1 and X2 are defined as the centroids for the alkene bonds of the COD co-ligand.

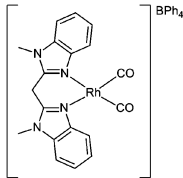
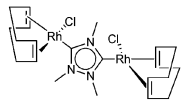
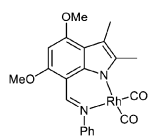
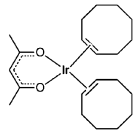
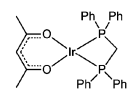
Based on the solid state structure of the imidazolyl complexes **5** and **6**, two unique imidazolyl donor environments were expected in the solution state. However, the ¹H NMR spectrum at room temperature only shows one set of resonances due to all three imidazolyl donors which suggests that the interconversion between the two binding modes (*i.e.* κ^2 and κ^3) is sufficiently fast measured on the NMR timescale such that all three imidazolyl donors become equivalent. The ¹H NMR spectrum of the complex $[\text{Rh}(\text{CO})_2(\text{tim})][\text{BArF}]$ (**6**) at –90 °C also did not resolve the resonances due to the imidazolyl donors in different chemical environments.

Intramolecular cyclization of aliphatic alkynoic acids to alkylidene lactones

It has been reported that changes in the steric environment induced by the three-dimensional arrangement of the ligand in a complex can induce changes in the selectivity and activity of the complex as a catalyst.²² In the previous sections, we have shown that in the solution state, the rhodium(I) complexes exist in a κ^2 binding mode, that is with two of the *N*-donors bound, while the third remains free in solution. The presence of the unbound *N*-donor could have a significant impact on the activity and selectivity of the complexes with tridentate ligands as catalysts relative to the activity of their counterparts with bidentate ligands.

The relative activity of the Rh(I) complexes **4a**, **4b** and **6** with tridentate pyrazole and imidazole ligands as catalysts was established for the intramolecular cyclization of 4-pentynoic acid (**8**) (Scheme 1 (a), Table 4). A solution of 4-pentynoic acid and 2 mol% of the catalyst in *d*₆-benzene was heated at 80 °C and the progress of the reaction monitored using ¹H NMR spectroscopy. Complexes **4a** and **4b** were not as active as catalysts for the intramolecular cyclization of **8** when compared to the imidazole-based complex **6**. In the case of **4a**, 1.4 h was required before complete conversion of starting material was observed (Table 4, entry 3), and for **4b**, 5.5 h was required before 78% conversion was observed (Table 4, entry 4). In the case of the imidazolyl complex (**6**), only 0.5 h was required under the same conditions to achieve complete conversion. The above results also suggest that the position of the amine group on the tpt complexes (*i.e.* **4a**, *para*; **4b**, *ortho*) has a significant influence on the activity of the complex as a catalyst for the intramolecular cyclization of 4-pentynoic acid (**8**). The reduced activity of the complex **4b** as a catalyst compared to

Table 4 Comparison of catalytic activity of rhodium(i) complexes and literature complexes as catalyst for the intramolecular cyclization of 4-pentynoic acid (**8**) to the corresponding lactone **9** (Scheme 1(a))

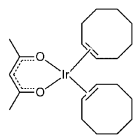
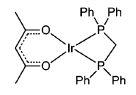
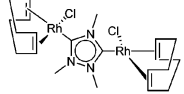
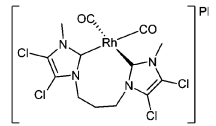
Entry	Catalyst	Mol% metal	Temperature, solvent	Time ^a
1	[Rh(bim)(CO) ₂][BARF] (7)	2	C ₆ D ₆ , 80 °C	0.3 h
2	[Rh(tim)(CO) ₂][BARF] (6)	2	—	0.5 h
3	[Rh(<i>p</i> -tpt)(CO) ₂][BARF] (4a)	2	—	1.4 h
4	[Rh(<i>o</i> -tpt)(CO) ₂][BARF] (4b)	2	—	5.5 h (78%)
5	[Rh(bim)(CO) ₂]BPh ₄	0.35	d ₆ -acetone, 50 °C	15.5 h ¹² (88%)
6		0.40	d ₆ -acetone, 50 °C	15.5 h ¹² (98%)
7		1	CD ₃ CN, 50 °C	8 h ¹³
8		2	CDCl ₃ , 60 °C	3 h ²³
9		5	CD ₃ CN, 25 °C	12 h ²⁴
10		5	CD ₃ CN, 25 °C	24 h ²⁴
11	AuCl + 10 mol% K ₂ CO ₃	10	CD ₃ CN, 24 °C	2 h ²⁵

^a Time required to achieve 100% conversion unless otherwise stated.

4a was attributed to steric interactions between the amine group and the substrate during the catalytic cycle, as both compounds are isoelectronic.

To determine the effect of the of the third unbound *N*-donor on catalytic activity, we studied the efficiency of the most active complex, [Rh(tim)(CO)₂][BARF] (**6**), and its counterpart, with a bidentate ligand [Rh(bim)(CO)₂][BARF] (**7**) as catalysts for the intramolecular cyclization of 4-pentynoic acid (**8**). Based on the percentage conversion of 4-pentynoic acid (**8**) to the corresponding lactone **9**, the rhodium(i) complex **7** with the bidentate ligand was the more efficient catalyst with complete conversion of substrate observed after 0.3 h compared to the 0.5 h required when complex **6** with the tridentate ligand was used as a catalyst. Presumably, the difference in the catalytic activity is due to the presence of the third unbound imidazolyl donor.

Table 5 Comparison of catalytic activity of rhodium(i) complexes and literature complexes as catalyst for the intramolecular cyclization of 5-hexynoic acid (**10**) to the corresponding lactone **11**

Entry	Catalyst	Mol% metal	Temperature, solvent	Time ^a
1	[Rh(bim)(CO) ₂][BARF] (7)	1	C ₆ D ₆ , 70 °C	13.3 h
2	[Rh(bim)(CO) ₂]BPh ₄	0.7	d ₆ -acetone 50 °C	192 h ¹² (80%)
3		5	CD ₃ CN, 25 °C	72 h ²⁴
4		5	CD ₃ CN, 25 °C	84 h ²⁴ (~80%)
5		1	CD ₃ CN, 50 °C	192 h ¹³
6		2	CDCl ₃ , 60 °C	168 h ²⁶ (15%)

^a Time required to achieve 100% conversion unless otherwise stated.

The presence of the third unbound imidazolyl limits the ability of the substrate to bind to the catalytic centre, or the nucleophilic attack of the oxygen nucleophile onto the activated alkyne bond. Despite the steric hindrance of the third unbound imidazolyl donor, the complex **6** is still active as a catalyst for the intramolecular cyclization of 4-pentynoic acids (**8**) compared to other complexes published previously (Table 4).

Based on the high activity of complex **7** as a catalyst for the intramolecular cyclization of 4-pentynoic acid (**8**), we examined the activity of complex **7** as a catalyst for the intramolecular cyclization of 5-hexynoic acid (Scheme 1 (b)). 5-Hexynoic acid (**10**) was heated at 70 °C in d₆-benzene in the presence of 1 mol% of **7** and the reaction monitored using ¹H NMR spectroscopy. Complete conversion of the alkyne acid **10** to the cyclic lactone **11** was observed after 13.3 h. This result is a considerable improvement over other literature reports of rhodium(i) complexes as catalysts for the same transformation (Table 5). In particular, this result also highlights the ability of a weakly coordinating counterion such as BARF (Table 5, entry 1) to improve catalytic performance of complexes compared to a coordinating counterion such as BPh₄ (Table 5, entry 2).¹⁴

Conclusion

A series of rhodium(i) complexes bearing the *p*- (**1a**) and *o*-tris(pyrazol-1-yl)toluidine ligands (**1b**) were synthesised and their coordination chemistry studied in the solid and solution state using X-ray crystallography and NMR spectroscopy, respectively. Despite the potential of the tris(pyrazol-1-yl)toluidine ligands to bind to the rhodium centre in either a κ² (bidentate)

or a κ^3 (tridentate) binding mode, the κ^2 binding mode was shown to be the preferred binding mode in the solid state for all of the complexes considered. Despite significant changes to the nature of the co-ligands (norbornadiene, 1,5-cyclooctadiene and carbon monoxide), it was found that the tris(pyrazol-1-yl)-toluidine ligand still favoured the κ^2 binding mode.

To investigate the influence of the donor strength of the tridentate ligands on the coordination chemistry of ligands, the analogous tris(*N*-methylimidazole-2-yl)methanol complexes [Rh(tim)(COD)][BARF] (**5**) and [Rh(tim)(CO)₂][BARF] (**6**) were synthesised and the structures of these complexes were also studied using X-ray crystallography and NMR spectroscopy. The rhodium(I) complexes **5** and **6** also adopted square planar geometries with a κ^2 binding mode. The bidentate binding mode of all of the complexes studied has important implications for their activity as catalysts, as the binding mode suggests that the complexes with tridentate ligands could behave in a similar fashion to the corresponding complexes with bidentate ligands.

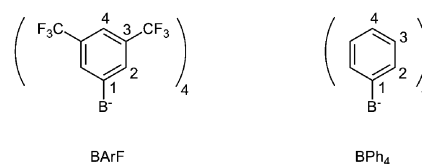
Of the three rhodium(I) complexes with tridentate *N*-donor ligands, the most active catalyst for the cyclisation of 4-pentynoic acid was the complex with the tridentate imidazolyl ligand, [Rh(tim)(CO)₂][BARF] (**6**). The activity of the complex **6** for the intramolecular cyclization of aliphatic alkynoic acids was compared with that of its counterpart bearing a bidentate ligand [Rh(bim)(CO)₂][BARF] (**7**), and it was found that the presence of the third unbound *N*-donor reduces the catalytic activity of the complex. This loss of activity is presumably due to the steric hindrance induced by the presence of an additional *N*-donor with the substrate during the catalytic cycle. Despite this loss of activity, the rhodium(I) complexes bearing the imidazolyl donor were shown to still be highly active in the intramolecular cyclization of aliphatic alkynoic acids compared to previously reported catalysts. We are currently also investigating the effect of the third ligand donor on the regioselectivity of the catalysed intramolecular hydroalkoxylation reaction.

Experimental

The preparation, purification and reaction of all complexes described were carried out using Schlenk techniques under an atmosphere of dry nitrogen using solvents dried using the PuraSolv solvent purifier system. The compounds [Rh(COD)₂][BARF],²⁷ [Rh(COD)Cl]₂,²⁸ [Rh(NBD)₂][BARF],²⁷ [Rh(bim)(CO)₂][BARF],¹⁰ 5-hexynoic acid,¹² *o*-tpt,⁹ *p*-tpt⁹ and tim²⁹ were prepared using literature methods. All organic compounds were purchased from Sigma Aldrich and used as received. Iridium(III) and rhodium(III) chloride hydrate were purchased from Precious Metals Online and used as received.

X-ray diffraction studies were performed on a Bruker APEXII diffractometer. All calculations were made with programmes of the SHELXTL system.³⁰ NMR spectra were recorded on Bruker Avance 400 or 600 MHz spectrometer using the residual solvent peak as reference. Microanalyses and high resolution mass spectrometry were carried out at the Mass Spectrometry service of the Research School of Chemistry, Australian National University, Canberra, Australia.

The numbering of the atoms within BARF⁻ and BPh₄⁻ counterions used is shown below.



General synthesis of rhodium bisolefin tris(pyrazol-1-yl)toluidine complexes bearing the BARF counterion. (**2**)

A solution of desired tris(pyrazol-1-yl)toluidine and [Rh(L)₂][BARF] (L = COD or NBD) in THF was stirred at room temperature for 20 to 30 min. The resulting solution was reduced *in vacuo* and the desired compound was recrystallised from a mixture of dichloromethane and *n*-pentane. Single crystals were grown *via* slow diffusion of *n*-pentane into a concentrated solution the desired complex in dichloromethane overnight at room temperature.

[Rh(*p*-tpt)(COD)][BARF] (2a**).** *p*-tris(pyrazol-1-yl)toluidine (**1a**) (28.4 mg, 0.10 mmol), [Rh(COD)₂][BARF] (103.6 mg, 0.09 mmol) to yield **2a** (103.6 mg, 75%) as yellow crystals (Found: C, 49.1; H, 3.1; N, 7.0%. C₅₆H₃₉BF₂₄N₇Rh requires C, 48.8; H, 2.6; N, 7.1%); δ_{H} (600 MHz; CDCl₃; -50 °C) δ 7.97 (br, 1H, H^{5P(2)} or H^{3P(2)}), 7.69 (br, 8H, H^{2BARF}), 7.49 (br, 4H, H^{4BARF}), 7.45 (br, 2H, H^{5P(1)} or H^{3P(1)}), 7.21 (br, 2H, H^{3P(1)} or H^{5P(1)}), 7.00 (br, 1H, H^{3P(2)} or H^{5P(2)}), 6.71 (d, *J* = 7.8 Hz, 1H, H^{3'}), 6.38 (br, 2H, H^{4P(1)}), 6.37 (br, 1H, H^{4P(2)}), 6.12 (d, *J* = 7.8 Hz, 1H, H^{2'}), 4.20 (br, 2H, H^{1,COD}), 3.64 (br, 2H, H^{1,COD}), 2.47 (br, 2H, H^{2,COD} or H^{3,COD}), 1.82 (br, 2H, H^{2,COD} or H^{3,COD}), 1.62 (br, 4H, H^{2,COD} and H^{3,COD}).¹³C{¹H} NMR (150 MHz; CDCl₃; -55 °C) 162.07 (q, *J* = 50 Hz, C^{1BARF}), 151.1 (C^{1'}), 146.1 (C^{3P(2)} or C^{5P(2)}), 143.6 (C^{3P(1)} or C^{5P(1)}), 135.63 (C^{3P(1)} or C^{5P(1)}), 135.14 (C^{2BARF}), 134.56 (C^{3P(2)} or C^{5P(2)}), 129.2 (q, *J* = 31 Hz, C^{3BARF}), 129.1 (C^{3'}), 124.9 (q, *J*_{C-F} = 270 Hz, CF₃), 123.9 (C^{4'}), 118.6 (C^{4BARF}), 117.9 (C^{1BARF}), 114.9 (C^{2'}), 108.9 (C^{4P(2)}), 108.1 (C^{4P(1)}), 94.2 (C^a), 84.2 (C^{1COD}), 83.60 (C^{1COD}), 30.63 (C^{2,COD} and C^{3,COD}), 29.67 (C^{2,COD} and C^{3,COD}).

[Rh(*o*-tpt)(COD)][BARF] (2b**).** *o*-tris(pyrazol-1-yl)toluidine (**1b**) (27.8 mg, 0.10 mmol), [Rh(COD)₂][BARF] (102.9 mg, 0.09 mmol) to yield **2b** (72.5 mg, 58%) as yellow crystals (Found: C, 48.6; H, 3.0; N, 6.5. C₅₆H₃₉BF₂₄N₇Rh requires C, 48.8; H, 2.6; N, 7.1%); δ_{H} (600 MHz; CDCl₃; -55 °C) 7.86 (br, 1H, H^{5P(3)}), 7.68 (br, 1H, H^{5P(2)}), 7.72 (br, 1H, H^{5P(1)}), 7.67 (s, 8H, H^{3BARF}), 7.57 (br, 1H, H^{3P(2)}), 7.52 (br, 1H, H^{3P(1)}), 7.48 (s, 4H, H^{1BARF}), 7.38 (t, *J* = 8.2 Hz, 1H, H^{4'}), 6.73 (t, *J* = 8.2 Hz, 1H, H^{3'}), 6.72 (br, 1H, H^{5'}), 6.69 (br, 1H, H^{4P(3)}), 6.52 (br, 1H, H^{4P(2)}), 6.40 (br, 1H, H^{4P(1)}), 5.52 (d, *J* = 8.2 Hz, 1H, H^{2'}), 4.31 (br, 1H, H^{1COD}), 4.26 (br, 1H, H^{1COD}), 3.90 (br, 1H, H^{1COD}), 3.73 (br, 1H, H^{1COD}), 2.66–2.51 (m, 1H, H^{2COD}), 2.50–2.40 (m, 1H, H^{2COD}), 2.08–1.67 (m, 1H, H^{2COD}), 1.96–1.77 (m, 4H, H^{2COD}), 1.77–1.62 (m, 1H, H^{2COD}). δ_{C} (150 MHz; CDCl₃; -50 °C) 161.2 (q, *J* = 49.3 Hz, C^{4BARF}), 144.9 (C^{3P(2)}), 144.8 (C^{3P(1)}), 143.4 (C^{1'}), 142.6 (C^{5P(3)}), 137.4 (C^{5P(2)}), 136.5 (C^{5P(1)}), 134.3 (C^{4'}), 134.0 (C^{3BARF}), 129.3 (C^{3P(3)}), 128.3 (q, *J* = 31 Hz, C^{2BARF}), 127.9 (C^{2'}), 124.0 (q, *J* = 271 Hz, CF₃), 119.6 (C^{3'}),

117.4 (C5'), 117.1 (C3^{BARF}), 114.6 (C1'), 109.3 (C4^{P3}), 108.9 (C4^{P1}), 108.4 (C4^{P2}), 92.1 (C^a), 86.3 (C1^{COD}), 83.8 (C1^{COD}), 82.8 (C1^{COD}), 30.4 (C2^{COD}), 29.9 (C2^{COD}), 29.3 (C2^{COD}), 28.8 (C2^{COD}).

[Rh(*p*-tpt)(NBD)][BARF] (3a). *p*-tris(pyrazol-1-yl)toluidine (1a) (44.0 mg, 0.10 mmol), [Rh(NBD)₂][BARF] (101.6 mg, 0.09 mmol) to yield 3a (119 mg, 98%) as yellow crystals (Found: C, 48.7; H, 2.7; N, 7.0. C₅₅H₃₅BF₂₄N₇Rh requires C, 48.5; H, 2.6; N, 7.2.); δ_H (600 MHz; CDCl₃; -55 °C) 7.99 (br, 1H, H5^{P(2)}), 7.69 (s, 8H, H2^{BARF}), 7.49 (s, 4H, H4^{BARF}), 7.17 (br, 2H, H5^{P(1)}), 7.14 (br, 2H, H3^{P(1)}), 7.09 (br, 1H, H3^{P(2)}), 6.69 (d, *J* = 8.2 Hz, 2H, H3'), 6.38 (br, 1H, H4^{P(2)}), 6.32 (br, 1H, H4^{P(1)}), 5.89 (d, *J* = 8.2 Hz, 2H, H2'), 4.03 (br, 2H, H1^{NBD}), 3.89 (br, 1H, H2^{NBD}), 3.51 (br, 2H, H1^{NBD}), 3.45 (br, 1H, H2^{NBD}), 1.17 (br, 2H, H3^{NBD}). δ_C (150 MHz; CDCl₃; -50 °C) 161.2 (q, *J*_{BC} = 49 Hz, C1^{BARF}), 149.9 (C4'), 145.0 (C5^{P(2)}), 142.1 (C3^{P(1)}), 134.4 (C5^{P(1)}), 134.3 (C2^{BARF}), 133.5 (C3^{P(2)}), 128.5 (q, *J* = 32 Hz, C3^{BARF}), 127.6 (C2'), 123.9 (q, *J*_{CF} = 271 Hz, CF₃), 123.4 (C1'), 117.2 (C4^{BARF}), 114.1 (C3'), 108.1 (C4^{P(2)}), 107.2 (C4^{P(1)}), 93.2 (C^a), 60.9 (C1^{NBD}), 59.3 (C1^{NBD}), 50.9 (C2^{NBD}), 50.4 (C2^{NBD}), 31.3 (C3^{NBD}).

[Rh(*o*-tpt)(NBD)][BARF] (3b). *o*-tris(pyrazol-1-yl)toluidine (1b) (43.5 mg, 0.10 mmol), [Rh(NBD)₂][BARF] (109 mg, 0.09 mmol) to yield 3b (111 mg, 91%) as yellow crystals (Found: C, 48.6; H, 2.4; N, 7.2. C₅₅H₃₅BF₂₄N₇Rh requires C, 48.5; H, 2.6; N, 7.2%); δ_H (400 MHz; CDCl₃; -55 °C) 7.75 (br, 1H, H5^{P(3)}), 7.74 (br, 1H, H5^{P(2)}), 7.65 (br, 1H, H5^{P(3)}), 7.69 (s, 8H, H2^{BARF}), 7.49 (s, 4H, H4^{BARF}), 7.36 (t, *J* = 8.2 Hz, 1H, H4'), 7.14 (br, 2H, H3^{P(3)} & H3^{P(2)}), 6.81 (d, *J* = 8.2 Hz, 1H, H5'), 6.70 (t, *J* = 8.2 Hz, 1H, H3'), 6.55 (br, 1H, H4^{P(1)}), 6.40 (br, 1H, H4^{P(2)}), 6.39 (1H, H4^{P(1)}), 6.20 (br, 1H, H3^{P(3)}), 5.55 (d, *J* = 8.2 Hz, 1H, H2'), 4.00 (s, 4H, H1^{NBD}), 3.81 (s, 2H, H2^{NBD}), 1.34 (s, 2H, H3^{NBD}). δ_C (100 MHz; CDCl₃; -55 °C) 161.9 (q, *J*_{BC} = 74 Hz, C1^{BARF}), 145.4 (C3^{P(3)} & C3^{P(2)}), 143.9 (C6'), 142.9 (C5^{P(3)}), 138.3 (C5^{P(2)}), 137.2 (C5^{P(1)}), 134.8 (C2^{BARF}), 134.6 (C4'), 128.7 (m, C3^{BARF}), 128.9 (C3^{P(3)}), 128.3 (C2'), 124.5 (q, *J*_{CF} = 271 Hz, CF₃), 119.6 (C3'), 117.9 (C5'), 117.7 (C4^{BARF}), 114.6 (C1'), 109.3 (C4^{P(1)}), 109.2 (C4^{P(3)}), 108.5 (C4^{P(2)}), 92.7 (C^a), 63.3 (C3^{NBD}), 61.0 (C1^{NBD}), 51.1 (C2^{NBD}).

General synthesis of rhodium dicarbonyl tris(pyrazol-1-yl)-aniline complexes (4a) and (4b)

A solution of the rhodium COD complex in dichloromethane was degassed using three consecutive cycles of freeze-pump-thaw and stirred under a carbon monoxide atmosphere for 30 to 60 min. To this solution, *n*-pentane was added and the resulting precipitate filtered and washed with *n*-pentane.

[Rh(*p*-tpt)(CO)₂][BARF] (4a). [Rh(COD)(*p*-tpt)][BARF] (2a) (185 mg, 0.14 mmol) to yield 4a (125 mg, 71%) as yellow crystals. δ_H (600 MHz; CDCl₃; -55 °C) 7.97 (br, 1H, H5^{P(2)}), 7.77 (br, 2H, H5^{P(1)}), 7.67 (s, 8H, H3^{BARF}), 7.48 (s, 4H, H1^{BARF}), 7.31 (br, 2H, H3^{P(1)}), 6.97 (br, 1H, H3^{P(2)}), 6.57 (d, *J* = 7.2 Hz, 2H, H3'), 6.44 (br, 2H, H4^{P(1)}), 6.35 (br, 1H, H4^{P(2)}), 6.00 (d, *J* = 7.2 Hz, 2H, H2'); δ_C (150 MHz; CDCl₃; -55 °C) 181.7 (CO), 181.2 (CO), 161.2 (q, *J* = 49 Hz, C4^{BARF}), 150.4 (C1'), 146.7 (C5^{P(1)}), 145.4 (C5^{P(2)}), 135.6 (C3^{P(1)}), 134.3 (C1^{BARF}),

133.8 (C3^{P(2)}), 128.3 (C2^{BARF}), 124 (CF₃), 117.2 (C3^{BARF}), 114.7 (C3'), 108.4 (C4^{P(2)}), 107.9 (C4^{P(1)}), 93.0 (C^a); *m/z* (ES⁺) 464.0350 (M⁺. C₁₈H₁₅N₇O₂Rh requires 464.0432). ν_{max}/cm⁻¹ (KBr) 3492(m), 3399(m), 3161(m), 3141(m), 2107(vs, νCO), 2046(vs, νCO), 1630(s), 1608(s), 1519(s).

[Rh(*o*-tpt)(CO)₂][BARF] (4b). [Rh(COD)(*o*-tpt)][BARF] (2b) (171 mg, 0.12 mmol) to yield 4b (131 mg, 80%) as yellow crystals. (Found: C, 45.0; H, 2.2; N, 6.9. C₅₀H₂₇BF₂₄N₇Rh requires C, 45.2; H, 2.1; N, 7.4%) δ_H (400 MHz; CDCl₃; -55 °C) 7.92 (d, *J* = 1.9 Hz, 1H, H3^{P(1)}), 7.86 (d, *J* = 3.0 Hz, 1H, H5^{P(1)}), 7.83 (d, *J* = 1.9 Hz, 1H, H3^{P(2)}), 7.81 (d, *J* = 3.0 Hz, 1H, H5^{P(2)}), 7.70 (d, *J* = 3.0 Hz, 1H, H5^{P(3)}), 7.67 (br, 4H, H1^{BARF}), 7.49 (br, 8H, H3^{BARF}), 7.40 (t, *J* = 8.2 Hz, 1H, H4'), 6.73 (t, *J* = 8.2 Hz, 1H, H3'), 6.63 (d, *J* = 2.5 Hz, 1H, H5'), 6.63 (t, *J* = 2.5 Hz, 1H, H4^{P(1)}), 6.50 (t, *J* = 2.5 Hz, 1H, H4^{P(2)}), 6.47 (t, *J* = 2.5 Hz, 1H, H4^{P(3)}), 6.44 (d, *J* = 2.5 Hz, 1H, H3^{P(3)}), 5.45 (d, *J* = 8.2 Hz, 1H, H2'). δ_C (100 MHz; CDCl₃; -55 °C) 181.8 (CO), 181.11 (CO), 161.7 (q, *J*_{BC} = 49 Hz, C4^{BARF}), 150.3 (C3^{P(1)}), 150.2 (C3^{P(2)}), 143.7 (C5^{P(3)}), 143.4 (C6'), 138.8 (C5^{P(1)}), 137.9 (C5^{P(2)}), 135.3 (C4'), 134.7 (C1^{BARF}), 129.3 (C3^{P(3)}), 128.9–128.3 (m, C2^{BARF}), 124.5 (q, *J*_{CF} = 273 Hz, CF₃), 120.2 (C3'), 118.0 (C5'), 116.4 (C3^{BARF}), 113.5 (C1'), 110.3 (C4^{P(3)}), 109.9 (C4^{P(1)}), 109.4 (C4^{P(2)}). ν_{max}/cm⁻¹ (KBr) 3504(m), 3415(m), 3165(m), 3145(m), 2104(vs, νCO), 2046(vs, νCO), 2015(m, νCO), 1632(s), 1609(s), 1575(m) and 1522(m).

[Rh(tim)(COD)][BARF] (5). A solution of tris(*N*-methylimidazol-2-yl)methanol (26.8 mg, 0.1 mmol) and [Rh(COD)₂][BARF] (101 mg, 0.09 mmol) in THF (5 mL) was stirred at room temperature for 20 to 30 min. The resulting pale yellow solution was reduced *in vacuo* and recrystallised from a mixture of dichloromethane and *n*-pentane to yield the 5 (81 mg, 70%) as a pale yellow solid. (Found: C, 47.2; H, 3.1; N, 6.4%. C₅₃H₄₀BF₂₄N₆ORh requires C, 47.3; H, 3.00; N, 6.2). δ_H (400 MHz; MeOD) δ 7.61 (12H, H2^{BARF} and H4^{BARF}), 7.25 (br, 3H, H2), 7.05 (br, 3H, H3), 4.10 (br, 4H, H1^{COD}), 3.76 (br, 9H, N-CH₃), 2.38–2.21 (m, 4H, H2^{COD}), 1.95–1.76 (m, 4H, H2^{COD}); δ_C (100 MHz; MeOD) 161.5 (q, *J* = 49 Hz, C1^{BARF}), 145.2 (C1), 134.4 (C2^{BARF}), 129.7–128.5 (m, C3^{BARF}), 126.0 (C3), 124.9 (C2), 124.4 (q, *J* = 271 Hz, CF₃), 117.6–116.6 (m, C4^{BARF}), 82.4 (d, *J* = 13.3 Hz, C1^{COD}), 35.0 (*N*-CH₃), 29.9 (C2^{COD}).

[Rh(tim)(CO)₂][BARF] (6). A solution of 6 (59.3 mg, 0.04 mmol) in dichloromethane (2 mL) was degassed using three consecutive cycles of freeze-pump-thaw was stirred under a carbon monoxide atmosphere for 30 to 60 min. To the solution, *n*-pentane was added and the resulting precipitate filtered and washed with *n*-pentane to yield the compound 6 (32.5 mg, 57%) as a bright yellow solid. δ_H (400 MHz; MeOD) 7.70–7.57 (m, 12H, H4^{BARF} & H2^{BARF}), 7.29 (d, *J* = 1.5 Hz, 3H, H2), 7.23 (d, *J* = 1.5 Hz, 3H, H3), 3.75 (s, 9H, N-CH₃); δ_C (100 MHz; MeOD) δ 183.9 (CO), 183.2 (CO), 161.4 (q, *J*_{BC} = 50 Hz, C1^{BARF}), 144.8 (C2), 134.4 (C2^{BARF}), 129.5–128.5 (m, C3^{BARF}), 128.8 (C3), 125.5 (C2), 124.4 (q, *J* = 271 Hz, CF₃), 117.3–116.9 (C2^{BARF}), 73.9 (C^a), 34.7 (*N*-CH₃). *m/z* (ESI⁺) 1295.1077 (M + H⁺. C₄₇H₂₉B₁₁N₆O₃F₂₄Rh requires 1295.1066). ν_{max}/cm⁻¹ (KBr) 3319(br), 3166(w), 3139(w), 2094(vs, νCO), 2032(vs, νCO), 1610(m), 1555(m), 1506(m), 1609(s).

Generalised procedure for metal catalysed intramolecular cyclisation of alkynoic acids. Catalysed intramolecular cyclisation of alkynoic acids was conducted on a small scale in NMR tubes fitted with a concentric Teflon valve. The catalyst precursor, the substrate and, if required, 2,6-dimethoxytoluene as an internal standard were dissolved in deuterated solvent. The temperature in the NMR spectrometer was calibrated using neat ethylene glycol and a K-type thermocouple. The identity of the product was confirmed by comparison with literature and/or identified using standard 2D NMR spectroscopic techniques. Unless otherwise stated in the results and discussion, the values quoted are the result of a single catalysis experiment.

Cyclisation of 4-pentynoic acid (8) to 5-methylenedihydrofuranone (9). The cyclisation of 4-pentynoic acid (8) (25 mg) to the corresponding lactone 9 was investigated using a series of catalysts (2 mol%) in deuterated benzene (0.5 mL). The progress of the reaction was monitored by ¹H NMR spectroscopy by comparing the integration of the resonances due to the alkyne proton of compound 9 relative to the appearance of the resonances due to the alkene proton of the lactone 9. The identity of the product was confirmed through comparison with literature spectroscopic data.¹²

Cyclisation of 5-hexynoic acid (10) to 5-methylenedihydropyranone (11). The catalysed cyclization of 5-hexynoic acid (10) (25 mg) to the corresponding lactone 11 was investigated using the complex 8 as catalyst (1 mol%) in deuterated benzene (0.5 mL). The progress of the reaction was monitored by ¹H NMR spectroscopy, comparing the integration of the resonances due to 2,6-dimethoxytoluene (internal standard) relative to the resonance due to the alkene proton of the lactone 11 with the integration of the resonance due to the alkyne proton relative to the internal standard at time zero. The identity of the product was confirmed through comparison with literature spectroscopic data.¹²

Acknowledgements

We would like to thank the University of New South Wales, the Australian Research Council, the Australian Government (APA) and Baxter Family Trust for funding. We would also like to acknowledge Dr Vicki Tolhurst and Dr Danielle Kennedy for their contributions.

Notes and references

- (a) B. A. Messerle and K. Q. Vuong, *Pure Appl. Chem.*, 2006, **78**, 385–390; (b) B. A. Messerle and K. Q. Vuong, *Organometallics*, 2007, **26**, 3031–3040; (c) D. F. Kennedy, A. Nova, A. C. Willis, O. Eisenstein and B. A. Messerle, *Dalton Trans.*, 2009, 10296–10304; (d) L. D. Field, B. A. Messerle, K. Q. Vuong and P. Turner, *Dalton Trans.*, 2009, 3599–3614.
- A. M. Trzeciak, B. Borak, Z. Ciunik, J. J. Ziolkowski, M. Fatima, S. C. G. Da and A. J. L. Pombeiro, *Eur. J. Inorg. Chem.*, 2004, 1411–1419.
- M. D. Ward, J. A. McCleverty and J. C. Jeffery, *Coord. Chem. Rev.*, 2001, **222**, 251–272.
- (a) D. L. Reger, *Comments Inorg. Chem.*, 1999, **21**, 1–28; (b) A. L. Rheingold, L. M. Liable-Sands and S. Trofimenko, *Inorg. Chem.*, 2000, **39**, 1333–1335; (c) A. L. Rheingold, C. D. Incarvito and S. Trofimenko, *Inorg. Chem.*, 2000, **39**, 5569–5571; (d) N. Burzlaff, I. Hegelmann and B. Weibert, *J. Organomet.*

- Chem.*, 2001, **626**, 16–23; (e) I. A. Guzei, K. Li, G. A. Bikzhanova, J. Darkwa and S. F. Mapolie, *Dalton Trans.*, 2003, 715–722; (f) C. Pettinari and R. Pettinari, *Coord. Chem. Rev.*, 2005, **249**, 663–691; (g) C. Pettinari and R. Pettinari, *Coord. Chem. Rev.*, 2005, **249**, 525–543; (h) S. O. Ojwach and J. Darkwa, *Inorg. Chim. Acta*, 2010, **363**, 1947–1964.
- (a) L. D. Field, B. A. Messerle, M. Rehr, L. P. Soler and T. W. Hambley, *Organometallics*, 2003, **22**, 2387–2395; (b) S. Burling, Leslie D. Field, Hsiu L. Li, Barbara A. Messerle and P. Turner, *Eur. J. Inorg. Chem.*, 2003, 3179–3184; (c) S. Burling, L. D. Field, H. L. Li, B. A. Messerle and A. Shasha, *Aust. J. Chem.*, 2004, **57**, 677–680; (d) H. R. Bigmore, S. C. Lawrence, P. Mountford and C. S. Tredget, *Dalton Trans.*, 2005, 635–651.
- (a) C. Copéret and J.-M. Basset, *Adv. Synth. Catal.*, 2007, **349**, 78–92; (b) Z. Wang, G. Chen and K. Ding, *Chem. Rev.*, 2008, **109**, 322–359.
- (a) T. Takahashi, T. Watahiki, S. Kitazume, H. Yasuda and T. Sakakura, *Chem. Commun.*, 2006, 1664–1666; (b) A. R. McDonald, H. P. Dijkstra, B. M. J. M. Suijkerbuijk, G. P. M. van Klink and G. van Koten, *Organometallics*, 2009, **28**, 4689–4699.
- (a) M. T. Reetz, M. Rentzsch, A. Pletsch, A. Taglieber, F. Hollmann, R. J. G. Mondiere, N. Dickmann, B. Hoecker, S. Cerrone, M. C. Haeger and R. Sterner, *ChemBioChem*, 2008, **9**, 552–564; (b) M. T. Reetz, *Top. Organomet. Chem.*, 2009, **25**, 63–92.
- B. J. Liddle and J. R. Gardinier, *J. Org. Chem.*, 2007, **72**, 9794–9797.
- S. L. Dabb, J. H. H. Ho, R. Hodgson, B. A. Messerle and J. Wagler, *Dalton Trans.*, 2009, 634–642.
- J. H. H. Ho, R. Hodgson, J. Wagler and B. A. Messerle, *Dalton Trans.*, 2010, **39**, 4062–4069.
- S. Elgafi, L. D. Field and B. A. Messerle, *J. Organomet. Chem.*, 2000, **607**, 97–104.
- E. Mas-Marza, E. Peris, I. Castro-Rodriguez and K. Meyer, *Organometallics*, 2005, **24**, 3158–3162.
- (a) C. Bruneau and P. H. Dixneuf, *Acc. Chem. Res.*, 1999, **32**, 311–323; (b) M. Beller, J. Seayad, A. Tillack and H. Jiao, *Angew. Chem., Int. Ed.*, 2004, **43**, 3368–3398; (c) I. Nakamura and Y. Yamamoto, *Chem. Rev.*, 2004, **104**, 2127–2198.
- C. Chapuis and D. Jacoby, *Appl. Catal., A*, 2001, **221**, 93–117.
- (a) D. M. T. Chan, T. B. Marder, D. Milstein and N. J. Taylor, *J. Am. Chem. Soc.*, 1987, **109**, 6385–6388; (b) T. B. Marder, D. Zargarian, J. C. Calabrese, T. H. Herskovitz and D. Milstein, *J. Chem. Soc., Chem. Commun.*, 1987, 1484–1485.
- R. A. Amos and J. A. Katzenellenbogen, *J. Org. Chem.*, 1978, **43**, 560–564.
- A. J. Hallett, K. M. Anderson, N. G. Connelly and M. F. Haddow, *Dalton Trans.*, 2009, 4181–4189.
- C. J. Adams, N. G. Connelly, D. J. H. Emslie, O. D. Hayward, T. Manson, A. Guy Orpen and P. H. Rieger, *Dalton Trans.*, 2003, 2835–2845.
- M. Brookhart, B. Grant and A. F. Volpe, *Organometallics*, 1992, **11**, 3920–3922.
- F. A. Cotton and J. L. Thompson, *Inorg. Chim. Acta*, 1984, **81**, 193–203.
- S. Das, G. W. Brudvig and R. H. Crabtree, *Chem. Commun.*, 2008, 413–424.
- J. H. H. Ho, D. S. C. Black, B. A. Messerle, J. K. Clegg and P. Turner, *Organometallics*, 2006, **25**, 5800–5810.
- M. J. Geier, C. M. Vogels, A. Decken and S. A. Westcott, *Eur. J. Inorg. Chem.*, 2010, 4602–4610.
- H. Harkat, A. Y. Dembelé, J.-M. Weibel, A. Blanc and P. Pale, *Tetrahedron*, 2009, **65**, 1871–1879.
- M. Viciano, E. Mas-Marzá, M. Sanaú and E. Peris, *Organometallics*, 2006, **25**, 3063–3069.
- B. Guzel, M. A. Omary, J. P. Fackler and A. Akgerman, *Inorg. Chim. Acta*, 2001, **325**, 45–50.
- J. Choudhury, S. Podder and S. Roy, *J. Am. Chem. Soc.*, 2005, **127**, 6162–6163.
- A. J. Canty, E. E. George and C. V. Lee, *Aust. J. Chem.*, 1983, **36**, 415–418.
- G. M. Sheldrick, *Acta Crystallogr., Sect. A: Found. Crystallogr.*, 2008, **A64**, 112–122.